III-V Membrane Devices Integrated on Si Photonics Platform

S. Matsuo, T. Fujii, T. Hiraki, T. Aihara, Y. Maeda, K. Takeda, and T. Segawa

NTT Device Technology Laboratories, 3-1 Morinosato-Wakamiya, Atsugi, Kanagawa 243-0198 Japan, shinji.matsuo@ntt.com

Abstract *We have developed InP-based membrane photonic devices on a Si photonics platform, enabling low power operation due to large optical confinement. Efficient optical coupling between InP and Si waveguides is achieved by using simple tapered waveguides. ©2023 The Authors*

Introduction

Heterogeneously integrated Si-based photonic integrated circuits (PICs) including III-V compound semiconductors have attracted much attention to achieve high throughput, low power consumption, and low cost. These devices are expected to be used not only for datacom applications, but also for computing and sensing applications. To fabricate such PICs, direct bonding technique is widely used [1]. In [1], heterogeneously integrated lasers are fabricated by a combination of direct bonding and proton ion implantation, in which the optical mode field is defined by a Si waveguide underneath a III-V die. This is well suited for manufacturing heterogeneously integrated Si-based PICs in Si CMOS fabs. These lasers are used as bias light for Si Mach-Zehnder modulators (MZMs) because of their high output power and high temperature operation [2].

The next step for heterogeneous PICs will be the direct modulation of III-V devices, as they offer high-efficiency modulation for both lasers and modulators. This requires high optical and carrier confinement using buried heterostructures (BH). However, it requires precise positional control between BH and Si waveguide. To solve this, we propose the epitaxial regrowth of III-V layers on InP thin film on Si substrate. This allows us to define the BH position by using the photolithographic makers on Si [3-5]. The key to achieving a high-quality epitaxial layer is the thickness of the III-V layer, which is less than the critical thickness of ~430 nm [4].

In this presentation, we will explain our recent results on heterogeneous integration of membrane III-V devices on SiO_2/Si substrates, such as directly modulated laser (DML) arrays [6] and external modulators [7,8]. We have heterogeneously integrated these devices using two fabrication methods: a combination of direct bonding and epitaxial regrowth, and micro-transfer printing (MTP) [9,10].

Membrane DML array fabricated by selective area growth method [6]

With their low power consumption, small footprint, and low cost, DMLs can be expected to be used for short-reach applications in data centres and supercomputers. In addition, wavelength division multiplexing (WDM) technology must be used to increase the transmission capacity per fibre.

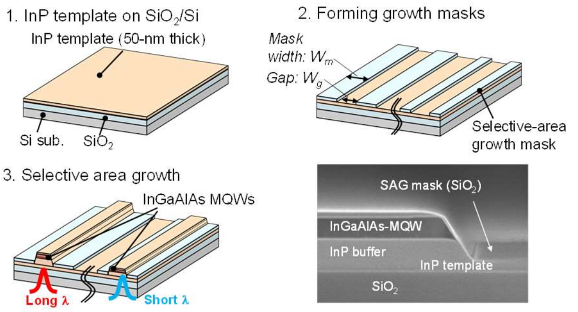

Fig. 1: Selective area growth process and cross-sectional SEM image of the MQW layer.

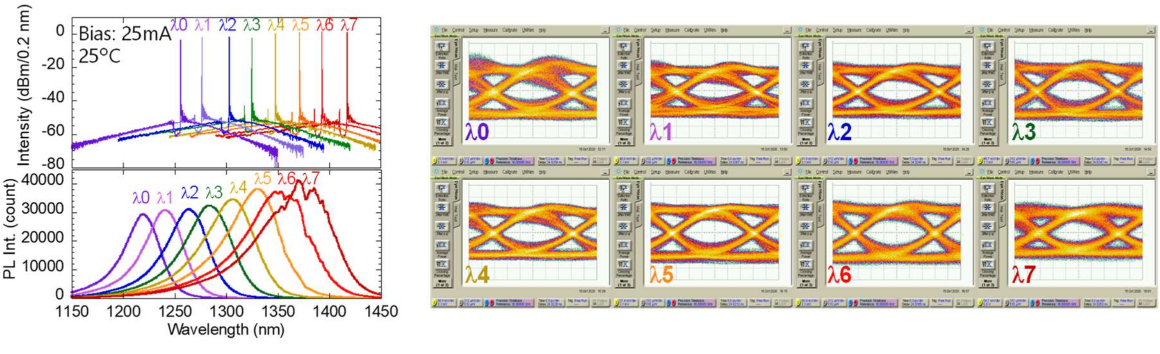

(a) (b)

Fig. 2: (a) PL spectra and lasing spectra for 8ch WDM DML array. (b) Eye diagrams with 32 Gbit/s NRZ modulation.

However, it requires different bandgap materials because the active region of the DML needs to be optimised to achieve high speed modulation with low power consumption.

To integrate different bandgap materials in a cost-effective way, we use selective-area growth (SAG), as shown in Fig. 1, where SiO_2 mask is formed on a 50-nm thick InP template on SiO_2/Si. In the SAG, the MQWs with different bandgaps are grown simultaneously by varying the SiO_2 mask width and gap. This is because the growth rate increases as the mask width increases and the gap decreases. Figure1 also shows a cross-sectional SEM image of the InGaAlAs-MQWs after SAG.

Figure 2 (a) shows photoluminescence (PL) and lasing spectra, where PL peak wavelength was changed more than 140 nm. To achieve this PL wavelength change, the SiO_2 mask width, W_m, ranged from 7 to 55 µm while the gap between the masks, W_g, was kept constant at 40 µm. By designing the grating pitch to account for the change in total III-V thickness due to SAGs, the lasing wavelengths of the DFB laser are also precisely controlled. Figure 3(b) shows the measured eye diagrams for 32-Gbit/s non-return-to-zero (NRZ) signals at 25°C. The bias current was ranged from 20.0 to 26.0 mA. We achieved 32-Gbit/s direct modulation for all eight-channel lasers.

Membrane EA-DFB laser [8]

Electro-absorption modulator (EAM) integrated DFB laser is also important for data centre networks because of its ultra-fast modulation speed and small footprint. Since the membrane structure on SiO_2/Si substrate has ultra-low parasitic capacitance, EAM on Si photonics platform provides 3-dB bandwidth over 50 GHz without using 50-Ω termination [8,11,12].

A schematic diagram of fabricated EA-DFB laser is shown in Fig. 3. The Si waveguide connects DFB laser and EAM sections. The laser section has the Si waveguide underneath the active region, which constructs optical supermode. On the other hand, there is no Si waveguide underneath the EAM section to increase the optical confinement factor. To connect each section with low propagation loss, InP tapered waveguide is used for DFB section and both InP and Si taper waveguides are used for the EAM section. A spot-size converter is used to connect high-NA fibres by combining the Si tapered waveguide and the SiO_x waveguide.

Figure 4 shows the lasing spectrum of the EA-DFB laser. The spectrum was observed from the laser monitor port as shown in Fig. 3. In the fabrication, we used the same active region for

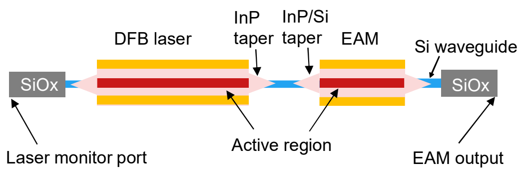

Fig. 3: Schematic diagram of fabricated EML.

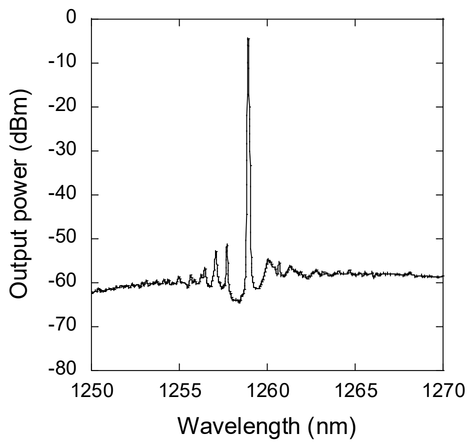

Fig. 4: Lasing spectrum of DFB laser.

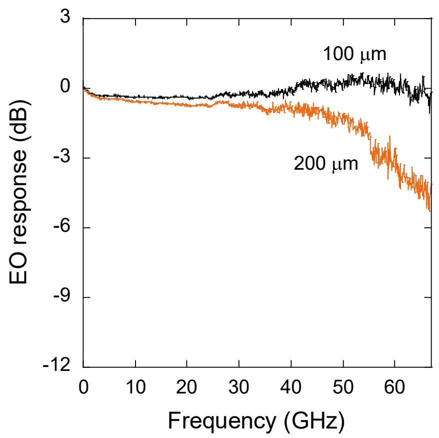

Fig. 5: Small signal responses of EAMs.

laser and EAM, and the length of the DFB laser and EAM was 300 µm and 100 µm, respectively. For a single mode lasing, we used a uniform SiN grating on the top surface of the InP layer and a width-modulated Si waveguide [13]. As shown in the figure, single-mode lasing was achieved with a side-mode suppression ratio (SMSR) of 48 dB at a laser bias current of 40 mA.

The small signal responses of the stand-alone EAMs were measured. The EAMs were 100 and 200 µm long, and the input wavelength and DC voltage were 1280 nm and 2 V, respectively. Thanks to the low parasitic capacitance of membrane EAMs, a 3-dB bandwidth above 67 GHz was observed for a 100-µm long EAM without using a 50-Ω termination.

We then measured a dynamic response of the

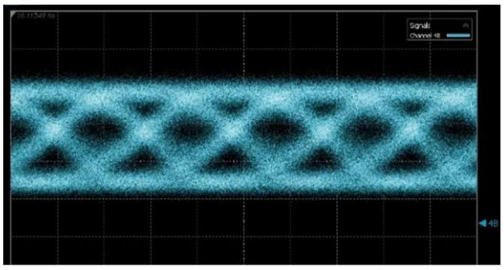

Fig. 6: Eye diagram of 112-Gbit/s NRZ signal.

EA-DFB laser. The eye diagram of the 112-Gbit/s NRZ signal with a 2-V DC bias is shown in Fig. 6. The LD current was 44 mA. We obtained a clear eye-opening with an extinction ratio (ER) of 3.2 dB.

Micro-transfer printed heterogeneously integrated membrane DML [9]

MTP has attracted much attention for heterogeneous integration on Si photonics platforms [14,15]. We believe this is particularly useful when the proportion of III-V devices occupied is small. Efficient optical coupling is easily achieved in membrane III-V devices, making MTP a suitable fabrication method for heterogeneous integration of membrane III-V devices on a Si photonics platform.

Figure 7 shows the optical microscope images of the fabricated membrane laser using MTP, where the membrane DML is aligned with a Si waveguide. We used a distributed-reflector (DR) laser consisting of a 140-µm-long DFB laser active section and a 60-µm-long DBR section. The output waveguide of the DML is an InP ridge waveguide and the optical coupling is achieved by reducing the width of the ridge waveguide as shown in the figure below.

I-L-V characteristics at room temperature is shown in Fig. 8. The threshold current was 1.2 mA. Mode hopping corresponding to reflection from the Si facet was observed.

Figure 9 shows the measured eye diagram of the 40-Gbit/s NRZ signal for a 2^{31}-1 pseudo-random bit sequence (PRBS). The bias current was 13.8 mA. A clear eye-opening was observed with the ER of 3.2 dB. The static and dynamic characteristics are no significant degradation to the use of MTP. Therefore, MTP is suitable for heterogeneous integration of membrane III-V devices on Si photonics platforms.

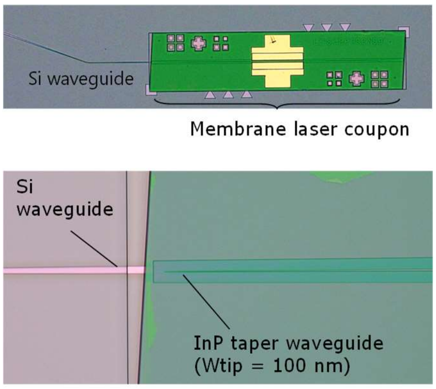

Fig. 7: Microscope images of the fabricated membrane DML using MTP.

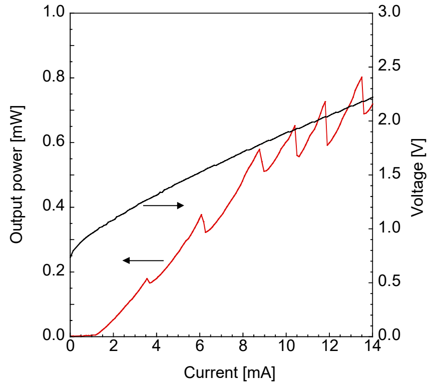

Fig. 8: I-L-V characteristic of fabricated device.

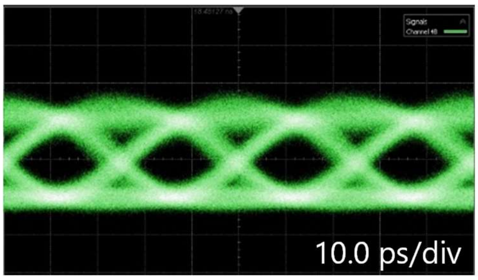

Fig. 9: Eye diagram of 40-Gbit/s NRZ signal.

Conclusions

We have developed the membrane III-V devices on Si photonics platform. These devices provide high modulation efficiency and easy to control optical mode profile between III-V and Si waveguides. In terms of device fabrication, we can use two fabrication methods, which are epitaxial growth on InP templated on Si substrate or micro-transfer printing. As a result, membrane III-V devices are expected to improve the performance of Si-based PICs.

Acknowledgement

We would like to thank Prof. Y. Arakawa, Prof. Y. Ota, and Prof. S. Iwamoto for the fruitful discussions on the MTP. We also thank M. Kiuchi, Y. Shouji, Y. Yokoyama, and K. Ishibashi for fabricating the devices.

References

[1] A. W. Fang, H. Park, O. Cohen, R. Jones, M. J. Paniccia, and J. E. Bowers, “Electrically pumped hybrid AlGaInAs-silicon evanescent laser,” Opt. Express, vol. 14, pp. 9203–9210, 2006, DOI: 10.1364/OE.14.009203.

[2] R. Jones, et al., "Heterogeneously Integrated InP/Silicon Photonics: Fabricating Fully Functional Transceivers," IEEE Nanotechnology Magazine, vol. 13, no. 2, pp.17 - 26, 2019,DOI: 10.1109/MNANO.2019.2891369

[3] S. Matsuo, T. Fujii, K. Hasebe, K. Takeda, T. Sato, and T. Kakitsuka, “Directly modulated buried heterostructure DFB laser on SiO_2/Si substrate fabricated by regrowth of InP using bonded active layer,” *Opt. Express*, vol. 22, no. 10, p. 12139, 2014, DOI: 10.1364/oe.22.012139.

[4] T. Fujii, T. Sato, K. Takeda, K. Hasebe, T. Kakitsuka, and S. Matsuo, “Epitaxial growth of InP to bury directly bonded thin active layer on SiO_2/Si substrate for fabricating distributed feedback lasers on silicon,” IET Optoelectronics, vol. 9, pp. 151–157, 2015, DOI: 10.1049/iet-opt.2014.0138.

[5] S. Matsuo, and T. Kakitsuka, “Low-operating-energy directly modulated lasers for short-distance optical interconnects,” Advances in Optics and Photonics, vol.10, no. 3, pp. 567-643, 2018, DOI: 10.1364/AOP.10.000567

[6] T. Fujii, K. Takeda, H. Nishi, N.-P. Diamantopoulos, T. Sato, T. Kakitsuka, T. Tsuchizawa, and S. Matsuo, “Multiwavelength membrane laser array using selective area growth on directly bonded InP on SiO_2/Si,” *Optica*, vol. 7, no. 7, p. 838, 2020, DOI: 10.1364/optica.391700.

[7] T. Hiraki, T. Aihara, T. Fujii, K. Takeda, T. Kakitsuka, T. Tsuchizawa, and S. Matsuo, “Membrane InGaAsP Mach–Zehnder Modulator Integrated With Optical Amplifier on Si Platform,” J. of Lightwave Technol. vol. 38, p. 3030, 2020, DOI: 10.1364/JLT.38.003030.

[8] T. Hiraki, T. Aihara, Y. Maeda, T. Fujii, T. Sato, T. Tsuchizawa, K. Takahata, T. Kakitsuka, and S. Matsuo, " Over-67-GHz-Bandwidth Membrane InGaAlAs Electro-Absorption Modulator Integrated With DFB Laser on Si Platform," J. of Lightwave Technol. vol. 41, pp. 880-887, 2023, DOI: 10.1109/JLT.2022.3221814.

[9] Y Maeda, et al., "Micro-Transfer-Printed Membrane Distributed Reflector Lasers on Si Waveguide Modulated With 50-Gbit/s NRZ Signal," J. of Lightwave Technol. vol. 41, pp. 880-887, 2023, DOI 10.1109/JLT.2023.3265973.

[10] S. Matsuo, T. Aihara, T. Hiraki, Y. Maeda, T. Kishi, T. Fujii, K. Takeda, and T. Kakitsuka, " Heterogeneously Integrated Membrane III-V Compound Semiconductor Devices with Silicon Photonics Platform," IEEE J. of Selected Topics in Quantum Electronics, vol. 29, p. 6100510, 2022, DOI: 10.1109/JSTQE.2022.3218297.

[11] S. A. Srinivasan, et al., “56 Gb/s germanium waveguide electro-absorption modulator,” J. Lightw. Technol., vol. 34, no. 2, pp. 419–424, 2016, DOI: 10.1109/JLT.2015.2478601.

[12] T. Hiraki et al., “50-GHz-bandwidth membrane InGaAsP electroabsorption modulator on Si platform,” J. Lightw. Technol., vol. 39, no. 16, pp. 5300–5306, 2021, DOI: 10.1109/JLT.2021.3082710.

[13] T. Aihara, T. Hiraki, T. Fujii, K. Takeda, T. Kakitsuka, T. Tsuchizawa, and S. Matsuo, " Membrane III-V/Si DFB laser using uniform grating and width-modulated Si waveguide," J. of Lightwave Technol. vol. 38, pp. 2961-2967, 2020, DOI 10.1109/JLT.2020.2978808.

[14] H. Yang, D. Zhao, S. Chuwongin, J.-H. Seo, W. Yang, Y. Shuai, J. Berggren, M. Hammar, Z. Ma, and W. Zhou, “Transfer-printed stacked nanomembrane lasers on silicon,” *Nature Photon. vol.* 6, no. 9, pp. 615–622, 2012, DOI: 10.1038/NPHOTON.202012.160.2978808.

[15] R. Katsumi, Y. Ota, M. Kakuda, S. Iwamoto, and Y. Arakawa, “Transfer-printed single-photon sources coupled to wire waveguides,” Optica vol. 5, pp. 691–694, 2018, DOI: 10.1364/OPTICA.5.000691.